Chen_Fig S1

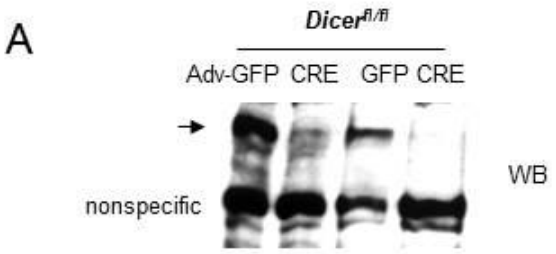
A
Dicer fl/fl
Adv-GFP CRE GFP CRE
nonspecific
WB

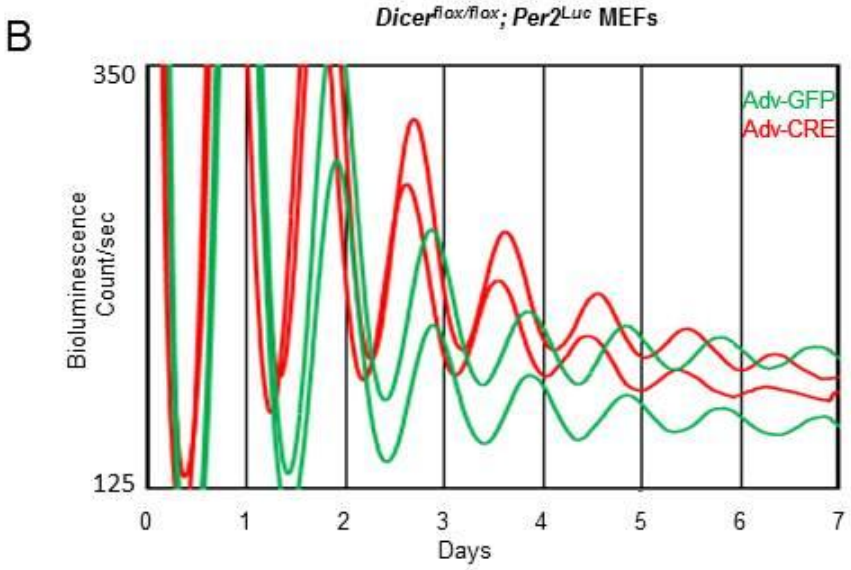
B
Dicer flox/flox; Per2 Luc MEFs
350
125
Bioluminescence Count/sec
Adv-GFP
Adv-CRE
0 1 2 3 4 5 6 7
Days

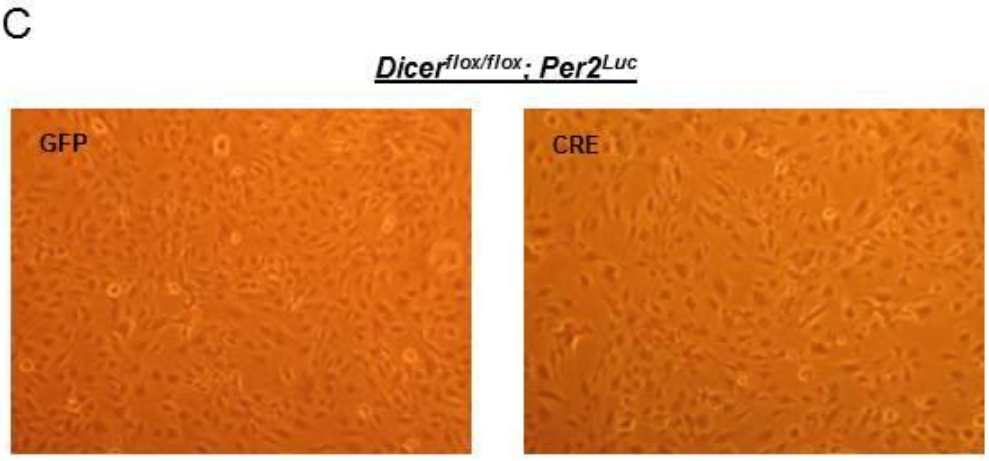
C
Dicer flox/flox; Per2 Luc
GFP
CRE

Chen_Fig S2

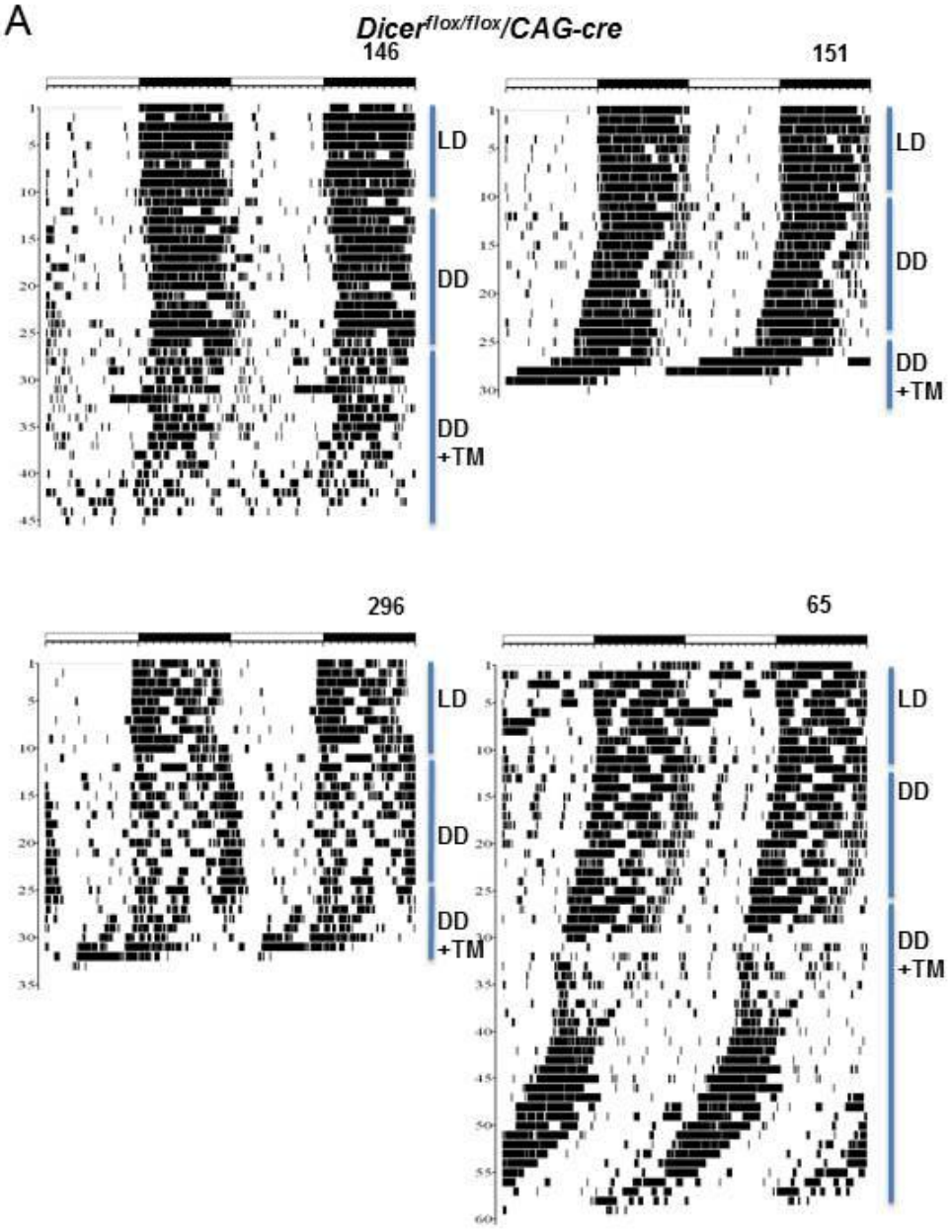
A
Dicer flox/flox/CAG-cre
146
151
296
65
LD
DD
DD
+TM

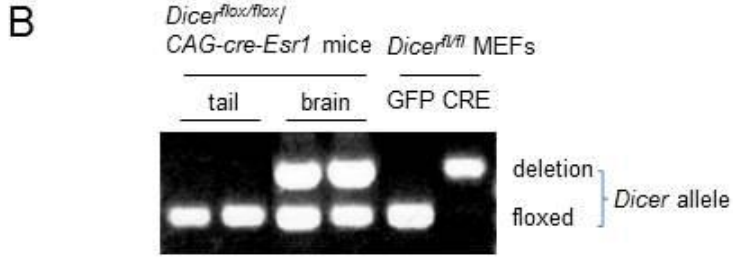
B
Dicer flox/flox/
CAG-cre-Esr1 mice
Dicer fl/fl MEFs
tail
brain
GFP
CRE
deletion
floxed
Dicer allele

Chen_Fig S3

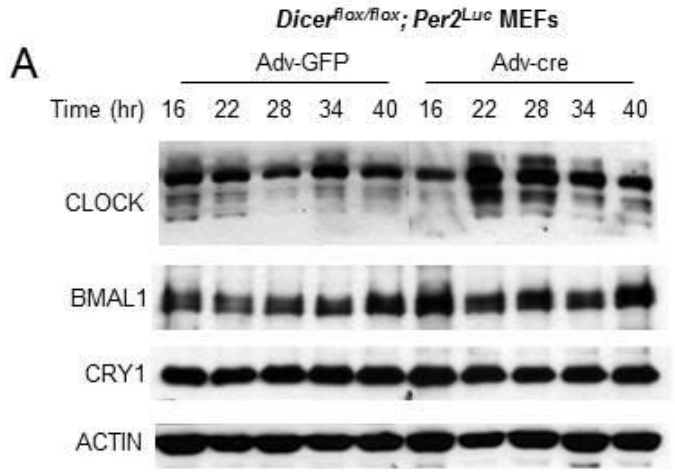
A
Dicer flox/flox; Per2 Luc MEFs
Adv-GFP
Adv-cre
Time (hr) 16 22 28 34 40 16 22 28 34 40
CLOCK
BMAL1
CRY1
ACTIN

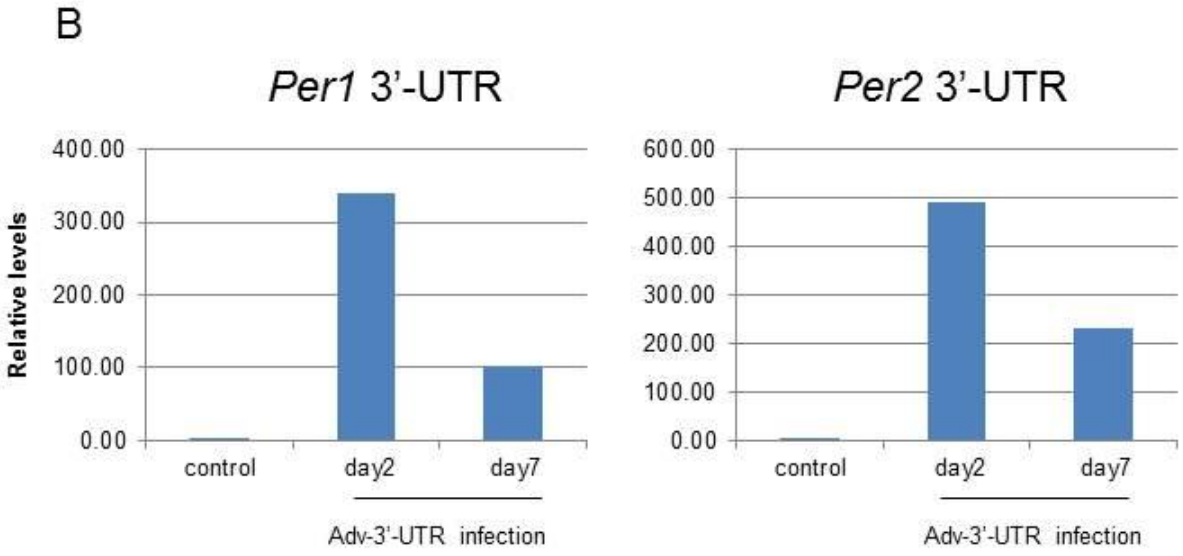
B
Per1 3'-UTR
Per2 3'-UTR
Relative levels
400.00
300.00
200.00
100.00
0.00
600.00
500.00
control
day2
day7
Adv-3'-UTR infection

Chen_Fig S4

Per1 3′-UTR *miRNA 24*

Per1 3′-UTR *miRNA 29*

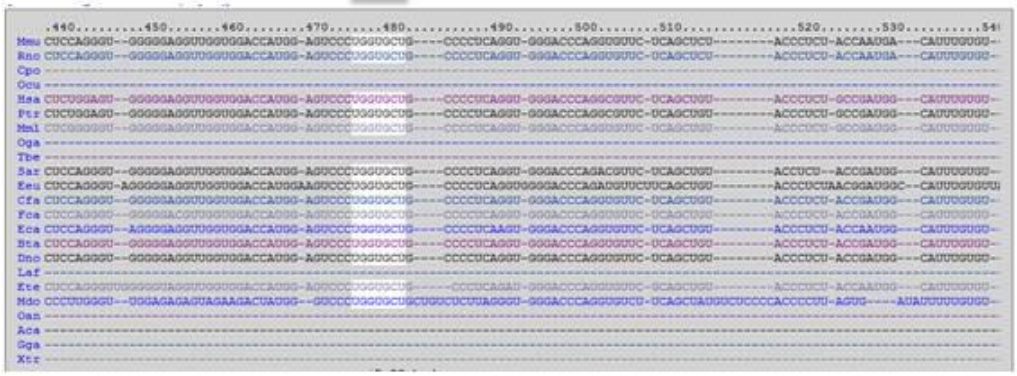

Per2 3′-UTR *miRNA 24*

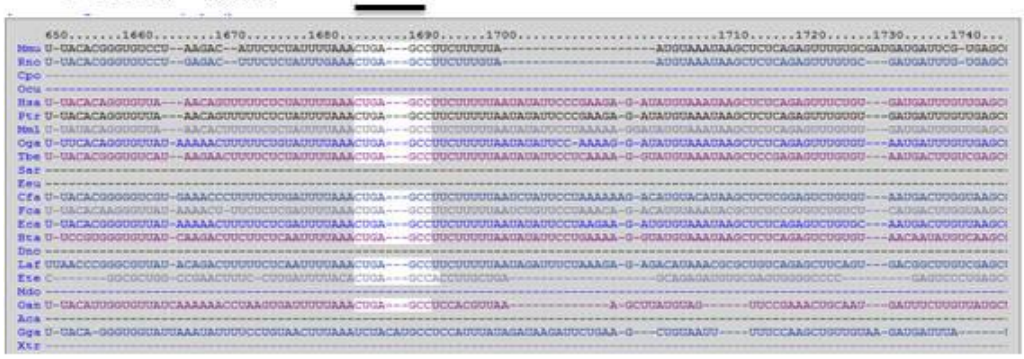

Per2 3′-UTR *miRNA 30*

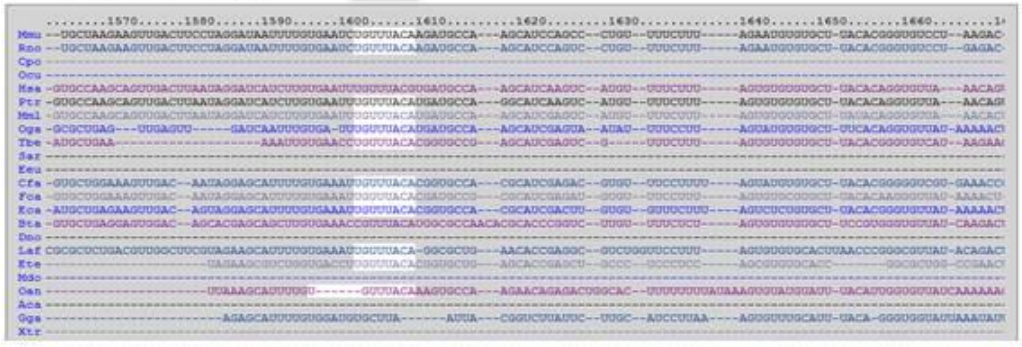

Chen_Fig S5

A

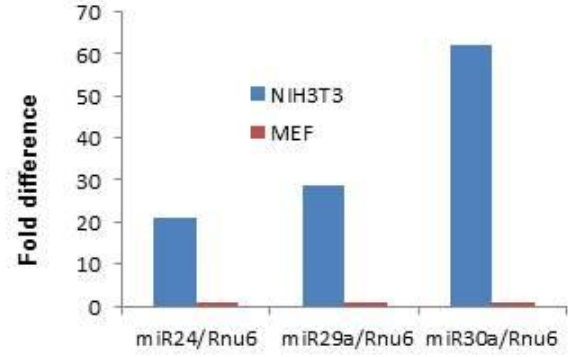

B

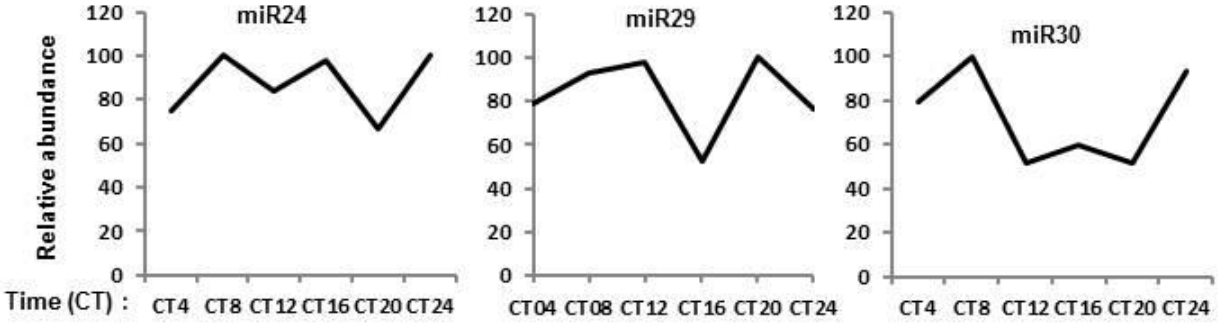

Fig S1, Related to Fig 1 and 2. Period is shortened in *Dicer*-deficient cells. (A) Immunoblots for Dicer. (B) Another experiment for bioluminescence rhythms in *Dicer*-mutant and control cells. (C) *Dicer*-mutant cells grow slowly. When floxed *Dicer* cells were plated onto final 35 mm dishes for recording bioluminescence rhythms after adenovirus infection followed by two passages, a smaller number of cells expressing CRE are present compared to cells expressing GFP. The same number of cells was used when the cells were infected with adenovirus.

Fig S2, Related to Fig 2. *Dicer*$^{flox/flox}$*/CAG-cre-Esr1* mice treated with tamoxifen exhibit gradual period shortening. (A) Mouse 151 was not included in the period calculation in Fig 2C because the mouse displayed locomotor activity only for several days and died prematurely in about a week after the tamoxifen treatment. (B) *Dicer* is deleted by the *CAG-cre-Esr1* transgenic driver in only half of brain cells. Tail DNA was prepared before the tamoxifen (TM) treatment, and brain DNA was recovered from the carcass of the same mice. Similar efficiency was observed for all other floxed *Dicer* constructs with the *cre* driver mice.

Fig S3, Related to Fig 3 and 5. *Per1* and *Per2* are major targets of miRNA-mediated regulation. (A) Levels of CLOCK, BMAL1 and CRY1 are not significantly altered in *Dicer* mutant cells compared to control cells. The samples used for PER immunoblots in Fig 3A were subjected to immunoblotting for these other clock proteins. (B) Exogenous *Per* 3'-UTR can be greatly overexpressed by the adenoviral vector in MEFs. MEFs were infected with adenovirus-*Per* 3'-UTR and harvested 2 and 7 days after the infection. Endogenous levels of *Per1* and *Per2* 3'-UTR in control cells were set to 1. Relative levels were calculated by RT-qPCR. Representative of two experiments.

Fig S4, Related to Fig 6A. miR-24 and 29a sites in the *Per1*-3'-UTR and miR-24 and 30a sites in the *Per2*-3'-UTR are conserved across many mammalian species. The alignments were generated using the TargetScanMouse algorithm.

Fig S5, Related to Fig 6B and 6E. Endogenous and exogenous miR-24, 29a, 30a expression in liver tissue and cells. (A) Relative endogenous expression levels between NIH 3T3 and MEFs. Levels of miRNAs relative to housekeeping control small RNA, Rnu6 were calculated in the cells. Rnu6 levels were comparable between the two types of cells. Levels in MEFs were set to 1. (B) miR-24, 29a and 30a do not show circadian oscillations. The analyses are representative of two experiments. Liver RNA samples were prepared at the indicated times and subjected to quantitative RT-PCR.

Table S1, Related to Fig 1. miRNAs are depleted in Dicer mutant cells. miR-24, 29a and 30a are highlighted in yellow in the table. Average absolute Ct values for miRNA 24, 29 and 30 family members are shown in the last table.